

Impulsive Light Scattering by Coherent Phonons in LaAlO₃: Disorder and Boundary Effects

Y. Liu,¹ A. Frenkel,¹ G. A. Garrett,^{1,2} J. F. Whitaker,¹ S. Fahy,³ C. Uher,^{1,2} and R. Merlin^{1,2,*}

¹Center for Ultrafast Optical Science, The University of Michigan, Ann Arbor, Michigan 48109-2099

²The Harrison M. Randall Laboratory of Physics, The University of Michigan, Ann Arbor, Michigan 48109-1120

³Department of Physics, University College, Cork, Ireland

(Received 8 December 1994)

Pump-probe measurements of coherent-phonon-induced changes of refractive index in LaAlO₃ are dominated by normally weak boundary effects. Atomic displacements in the range 50–500 μÅ were generated and probed by femtosecond laser pulses through impulsive Raman scattering. The absence of a bulk contribution is ascribed to phase mismatch due to domain disorder. Selection rules are consistent with a Raman model considering reflection and transmission at interfaces. Intensities and phonon parameters as a function of temperature agree well with incoherent Raman data.

PACS numbers: 78.47.+p, 63.20.-e, 78.30.Hv, 77.84.-s

It has become possible in recent years to generate coherent optical phonons through impulsive stimulated scattering (ISS) by using ultrashort high intensity light pulses [1–10]. This has provided a unique tool for time-domain studies of high-frequency modes and their coupling to electronic degrees of freedom and other excitations [1–9]. These developments have also lead to intriguing proposals bearing on the potentially large amplitude atomic motion that can be attained with ISS [10]. In this Letter, we report on the first observation of *boundary* contributions to ISS. Although particularly important in regard to measurements of the absolute cross section, these terms have not been previously considered theoretically or experimentally. Boundary effects distinguish themselves in that the phase of the ISS signal is shifted by $\pi/2$ with respect to that for the bulk. Our results were obtained on the antiferroelectric LaAlO₃. This compound does not exhibit bulk terms because of phase mismatch due to domain disorder. We also present a detailed analysis of the phonon oscillations and ISS selection rules, as well as a comparative study with spontaneous Raman scattering (RS) showing very good agreement with theoretical predictions.

LaAlO₃ undergoes a nearly second-order transformation at $T_C \approx 750$ K from the cubic perovskite structure (O_h) into a rhombohedral form (D_{3d}) [11]. The transition is characterized by the softening of a phonon at the R point of the cubic Brillouin zone and concomitant doubling of the unit cell. Below T_C , the R point becomes the Γ point of the D_{3d} phase where the soft phonon splits into Raman-allowed modes of symmetries A_{1g} and E_g (note that these *gerade* representations are not infrared active [12]). Our work concentrates on the latter optical vibrations. The LaAlO₃ sample was a single crystal $\approx 10 \times 10 \times 0.5$ mm³ platelet oriented along [001] (we use the pseudocubic indexing). Consistent with other studies [13], an examination using polarized optical microscopy reveals a structure of domains with {100} twin boundaries perpendicular to the surface. The twins correspond to the four equivalent $\langle 111 \rangle$ orientations of the rhombohedral (optical) axis.

ISS measurements at temperatures $T \approx 10$ –300 K were performed using a standard pump-probe setup, as sketched in Fig. 1. The pump beam, chopped at 2 MHz, was focused normal to the sample (001) surface to a 70-μm-diam spot while the probe beam was focused at $\approx 5^\circ$ incidence to a slightly smaller spot. Transform-limited 75–100 fs pulses at a repetition rate of 76 MHz, average power $\langle P \rangle \approx 200$ –400 mW and central wavelength $\lambda_L = 7900$ Å, were generated by a Ti-sapphire laser. RS data with ~ 0.5 cm⁻¹ resolution were obtained using a

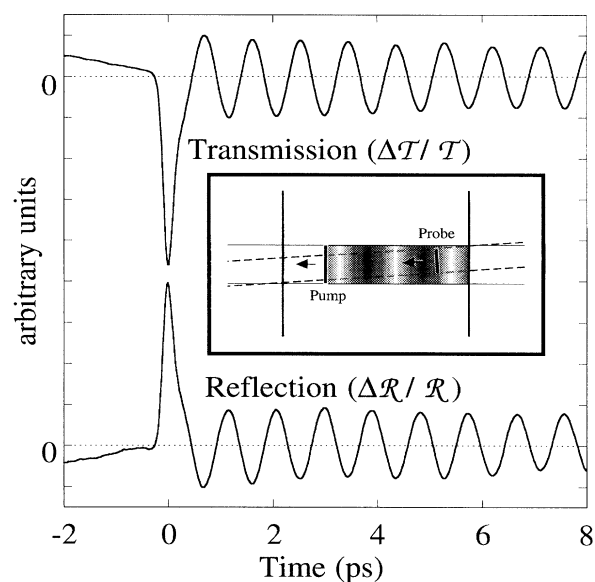


FIG. 1. Transmission ($\Delta\mathcal{T}/\mathcal{T}$) and reflection ($\Delta\mathcal{R}/\mathcal{R}$) geometry data ($T = 21$ K). The pump and probe beam are polarized along [010] and [100], respectively. $\langle P \rangle_{\text{pump}} = 13$ mW and $\langle P \rangle_{\text{probe}} = 40$ mW. The inset shows a schematic snapshot diagram of the ISS experiment. Dimensions scale approximately with those of the actual measurements. The gray scale represents the phonon displacement field, which moves with and is generated by the pump. In the time-resolved data the transmitted or reflected intensity of the probe pulse is plotted as a function of the time delay between the two pulses.

TABLE I. Raman susceptibility tensors $\partial\chi_{kl}/\partial Q$ (pseudocubic axes) and experimental values; the trigonal axis is along [111]. The conventional D_{3d} components [16] are given by the relations $a = (a' - b')$, $b = (a' + 2b')$, $d = 3d'$, and $e = \sqrt{6}e'$.

$A_{1g}(\Gamma_1^+)$ ($\text{cm}^{1/2} \text{g}^{-1/2}$)		$E_g(\Gamma_3^+)$ ($\text{cm}^{1/2} \text{g}^{-1/2}$)
$\begin{bmatrix} a' & b' & b' \\ b' & a' & b' \\ b' & b' & a' \end{bmatrix}$	$\frac{1}{\sqrt{3}} \times$	$\begin{bmatrix} 3d' + 2e' & 2e' & -3d' \\ 2e' & -3d' + 2e' & 3d' - e' \\ -3d' & 3d' - e' & -4e' \end{bmatrix} \begin{bmatrix} d' - 2e' & -2d' & d' - e' \\ -2d' & d' + 2e' & d' + e' \\ d' - e' & d' + e' & -2d' \end{bmatrix}$
$ a' = (6.1 \pm 1.8) \times 10^7$		$ d' = (5.5 \pm 0.9) \times 10^7$
$ b' = (5.5 \pm 1.5) \times 10^7$		$ e' = (5.2 \pm 1.5) \times 10^7$

Spex 1403 spectrometer and 30 mW of the 6471-Å Kr line. Spectra were recorded in the $z(x, x)z$ and $z(x, y)z$ near forward-scattering configurations where z is normal to (001) and x, y are along the [100] and [010] directions.

In the experiments a phonon wave created impulsively by the pump modifies the refractive index for the probe pulse which follows behind. The equations describing the coupled coherent phonon and electromagnetic fields are [14,15]

$$\ddot{Q}_s(\mathbf{r}, t) + \Gamma \dot{Q}_s(\mathbf{r}, t) + \frac{1}{8\pi^3} \int \omega_{\mathbf{q}}^2 e^{-i\mathbf{q}\cdot(\mathbf{r}-\mathbf{r}')} \times Q_s(\mathbf{r}', t) d^3\mathbf{r}' d^3\mathbf{q} = \frac{1}{2} \left(\sum_{kl} \frac{\partial \chi_{kl}^{(s)}}{\partial Q_s} \mathcal{E}_k \mathcal{E}_l^+ \right), \quad (1)$$

$$\nabla^2 \mathcal{E}_k = \frac{1}{c^2} \frac{\partial^2}{\partial t^2} \left(n^2 \mathcal{E}_k + 4\pi \sum_{ls} \frac{\partial \chi_{kl}^{(s)}}{\partial Q_s} Q_s \mathcal{E}_l \right). \quad (2)$$

Here, $Q_s = V^{-1/2} \sum_{\mathbf{q}} Q_{\mathbf{q}}^s \exp(i\mathbf{q}\cdot\mathbf{r})$ is the phonon field; $Q_{\mathbf{q}}^s$ denotes the amplitude of the s th component of the normal mode of wave vector \mathbf{q} and frequency $\omega(\mathbf{q})$, and V is the volume. Dissipation is accounted for phenomenologically by the term involving Γ . \mathcal{E}_k are electric field components and $n = 2.09 \pm 0.06$ at 7900 Å is the refractive index (we ignore the weak birefringence of LaAlO_3). $\partial\chi_{kl}/\partial Q$ is the Raman susceptibility; the relevant A_{1g} ($s = 1$) and E_g ($s = 1, 2$) irreducible tensors for LaAlO_3 are listed in Table I [16].

Let $\mathcal{E}_k = E_0 \cos(\alpha_k) G(t')$ and $e_k = e_0 \cos(\beta_k) G(t' - \delta)$ with $t' = t - zn/c$ be, respectively, the bare pump and probe pulses propagating along $z \equiv [001]$; α_k and β_k define the polarization directions and $\delta > 0$ is the delay. For a Gaussian-shaped pulse, $G(t) = \exp[-(t^2/2\tau^2)] \cos(2\pi ct/\lambda_L)$, and ignoring field depletion and phonon dispersion, the solution to (1) in the limit $|e_0| \ll |E_0|$, $\tau \ll t'$, and $\Gamma\tau \ll 1$ is [15]

$$Q_s(t') \approx \frac{\pi^{1/2}\tau}{4\omega} |E_0|^2 e^{-\omega^2\tau^2/4} \times \left(\sum_{kl} \frac{\partial \chi_{kl}^{(s)}}{\partial Q_s} \cos(\alpha_k) \cos(\alpha_l) \right) e^{-\Gamma t'/2} \sin(\tilde{\omega} t'), \quad (3)$$

where $\tilde{\omega} = (\omega^2 - \Gamma^2/4)^{1/2}$. For a slab of thickness h , the phonon-induced relative change in the probe-pulse intensity is [15]

$$\sum_k \int |\tilde{e}_k|^2 dt' / \sum_k \int |e_k|^2 dt' - 1 \approx -\frac{h\sigma}{c} e^{-\Gamma\delta'/2} \cos(\omega\delta'), \quad (4)$$

with

$$\sigma = \frac{\pi^{3/2}\tau}{2n} |E_0|^2 e^{-\omega^2\tau^2/2} \times \sum_{kl, mp, s} \left[\frac{\partial \chi_{mp}^{(s)}}{\partial Q_s} \cos(\alpha_m) \cos(\alpha_p) \times \frac{\partial \chi_{kl}^{(s)}}{\partial Q_s} \cos(\beta_k) \cos(\beta_l) \right] \quad (5)$$

and $\delta' = \delta - \tau^2\Gamma/2$; \tilde{e}_k are the components of the modified probe beam. These expressions are valid for $\Gamma \ll \omega$. Here, the main result is that the dependence of the probe-beam intensity on the delay δ' is determined by the Raman shift, i.e., the phonon frequency. Other than for a trivial renormalization of the probe intensity [15], Eq. (4) also applies to arbitrary values of the ratio $|e_0|/|E_0|$. The modulation is $\propto h$ because of perfect phase matching. The term $\cos(\omega\delta')$ reflects the fact that energy transfer between the probe impulse and the phonon field is largest at $Q = 0$ [15].

The above result represents the *bulk* contribution to ISS. A more complete solution, including the effect of the boundaries at $z = 0$ and $z = h$, contains the additional term [17]

$$\Delta\mathcal{T}/\mathcal{T} \approx \frac{2\sigma(n-1)}{\omega n(n+1)} e^{-\Gamma\delta'/2} \sin(\omega\delta') \quad (6)$$

independent of h ; \mathcal{T} is the transmitted probe intensity. Further, one can show that the coherent vibration leads also to a modulation of the intensity \mathcal{R} of the probe pulse reflected at $z = 0$ with [17]

$$\Delta\mathcal{R}/\mathcal{R} \approx -\frac{4\sigma}{\omega(n-1)(n+1)} e^{-\Gamma\delta'/2} \sin(\omega\delta'). \quad (7)$$

Qualitatively, interface and bulk contributions differ in that the latter reflects primarily the modulation of the transmitted beam *phase* by the phonon ($\propto h$) while (6) and (7) are nothing more than derivatives with respect to n of the transmitted and reflected pulse *amplitudes*. These differences lead to the $\pi/2$ phase shift distinguishing the

two components. It is clear that the boundary terms do not depend on h for short enough pulses.

Our low-temperature ISS results, shown in Figs. 1 and 2, disagree with (4) but are consistent with boundary effects. The traces in Fig. 1 exhibit weakly damped oscillations of period ≈ 1 ps preceded by a pronounced

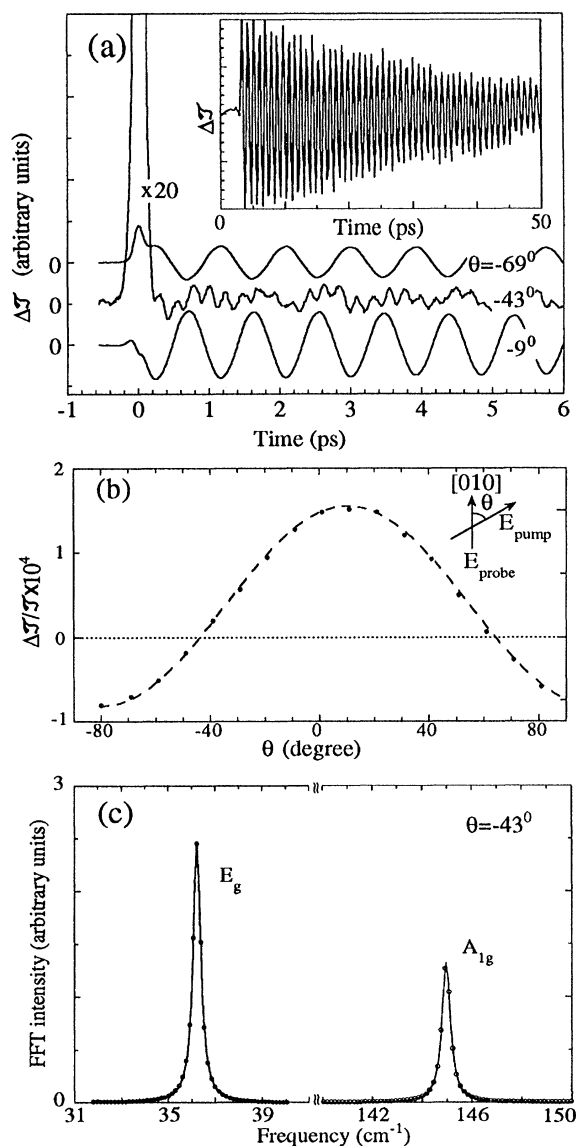


FIG. 2. ISS data (transmission geometry) at $T = 21$ K and $\langle P \rangle_{\text{pump}} = 26$ mW. The probe beam is polarized along [010]. (a) Spectra as a function of the angle θ between the probe and pump polarization, $\langle P \rangle_{\text{probe}} = 18$ mW. The main oscillations are due to the E_g mode at 36 cm^{-1} . Results at $\theta = -43^\circ$ show beating between the latter and the 145 cm^{-1} A_{1g} phonon. Data at long times for $\theta = 11^\circ$ and $\langle P \rangle_{\text{probe}} = 39$ mW are shown in the inset. (b) Relative transmission change vs θ , the dashed curve is a guide to the eye. (c) FFT spectrum corresponding to the ISS results of (a), solid lines are Lorentzian fits.

feature which we assign to the so-called coherent artifact [18]. The latter provided us with an accurate determination of zero time delay for $\delta - \delta' \ll \tau$. The oscillations are due to the varying refractive index which accompanies the phonon wave; their period agrees extremely well with that of the soft E_g mode [12] determined from RS spectra (see below). Careful analyses indicate that $\Delta\mathcal{T}$ and $\Delta\mathcal{R}$ vanish at $\delta'\omega = p\pi$ (integer p) in accordance with (6) and (7). The experiments also follow the prediction that the phase difference between $\Delta\mathcal{T}$ and $\Delta\mathcal{R}$ is $\approx \pi$. However, the calculated ratio between $\Delta\mathcal{R}/\mathcal{R}$ and $\Delta\mathcal{T}/\mathcal{T}$ is a factor of 4 larger than the measured value (the bulk expression *underestimates* this ratio by a factor of 10). Tentatively, we attribute the discrepancy to an experimental artifact arising from imperfect overlap between the pump and probe beams.

The symmetry rules which manifest themselves in the $\Delta\mathcal{T}$ vs θ data of Fig. 2 confirm the ISS origin of the oscillations; θ is defined in the inset of Fig. 2(b). Following (5) and the E_g tensors of Table I, it can be shown [17] that while the dependence of σ on θ varies with the domain orientation, values at $\theta = 0^\circ$ and $\theta = 90^\circ$ are not affected by twinning. The calculations give $\sigma(0^\circ)/\sigma(90^\circ) = -2$, in good agreement with the experiments. We emphasize that the E_g angular dependence is a function of the rhombohedral-axis coordinates, so that the behavior observed in Fig. 2(b) represents an average over many domains. At angles for which $\Delta\mathcal{T}(E_g) \approx 0$, the traces exhibit beating between the E_g and a higher-frequency oscillation (period ≈ 0.25 ps) due to the A_{1g} component of the soft phonon [12]; see Fig. 2(a) at $\theta = -43^\circ$ and Fig. 2(c). Consistent with (6), $\Delta\mathcal{T}(A_{1g}) \approx 0$ for $\delta\omega = p\pi$ (integer p).

The results for the E_g phonon reproduced in Fig. 3 and the comparison between ISS and RS spectra provide additional support for our interpretation. As shown in Fig. 3(a) for ISS and Fig. 3(b) for RS, ω decreases with increasing T while Γ increases. The data of Fig. 3(b) (inset) and Fig. 3(c) indicate that phonon parameters from RS and ISS are in excellent agreement and, thus, that our ISS measurements probe the linear regime. From the RS spectra (not shown for A_{1g}), relative values of the E_g and A_{1g} tensor components can be easily determined, given that our configuration intensities do not depend on the rhombohedral axis orientation. The absolute values of the Raman susceptibility listed in Table I were gained from (6) and (7) using measurements of $\Delta\mathcal{T}(E_g)/\mathcal{T}$ together with intensity ratios from RS. Considering that the factor $\exp(-\omega^2\tau^2/2)$ in (5) strongly suppresses A_{1g} but not E_g ISS, it is reassuring that values of $\partial\chi_{kl}/\partial Q$ inferred from RS and ISS are the same for $\tau \sim 120$ fs, in reasonable agreement with the measured pulse width. The data of Table I and (3) lead to 0.6 – 6 $\text{m}\mathring{\text{A}}/(\text{Jm}^{-2})$ for the ratio between the coherent vibration amplitude and the pulse energy areal density. This translates into 50 – 500 $\mu\mathring{\text{A}}$ displacements for our range of parameters.

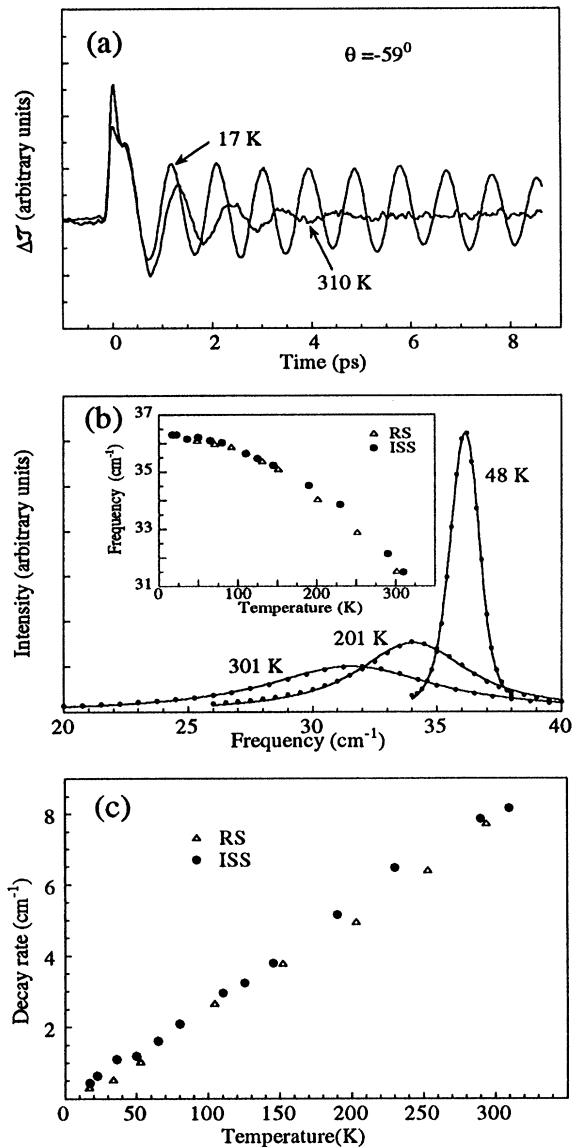


FIG. 3. Temperature dependence. For ISS, $\langle P \rangle_{\text{pump}} = 26$ mW and $\langle P \rangle_{\text{probe}} = 4$ mW; for RS, $P = 30$ mW and $\lambda_L = 6471$ Å. (a) ISS data (transmission geometry). (b) Incoherent E_g Raman spectra, solid lines are Lorentzian fits. The inset compares ISS and RS results on the temperature dependence of $\omega(E_g)$. (c) $\Gamma(E_g)$ vs T .

The fact that the bulk contribution (4) is lacking cannot be explained by phase mismatch due to either bulk birefringence or linear susceptibility dispersion; our measurements indicate that these effects are negligible in LaAlO_3 . Instead, we propose that the absence of the term $\propto h$ is the result of random phase shifts reflecting changes in the refractive index associated with the various domain orientations. These shifts introduce a length scale for the Raman polarization and, thus, for phase mismatch of the order of the domain size ℓ . It follows that the

condition for domain-related disorder to strongly reduce the bulk intensity while having little impact on interface components is $\lambda_L/n \ll \ell \ll h$. With $\ell \sim 10$ μm [13], it is clear that the latter is well satisfied by our ISS experiments (since phonon dispersion in the relevant wave vector range is negligible, such a disorder scale will have little effect on RS spectra). In the domain-disorder scenario, the relative phase of the phonon oscillation at the two boundaries is not well defined (however, notice that the delay between the probe and the phonon wave does not depend on the disorder since the pump and probe pulses follow identical paths). Whereas this has little impact on boundary contributions relying on the behavior in the immediate vicinity of the interfaces, the randomness modifies the bulk scattering representing an integrated effect over the total length of the sample.

We thank S. Y. Hou and J. M. Phillips for providing us with LaAlO_3 samples. This work was supported by the National Science Foundation through the Center for Ultrafast Optical Science under STC PHY 8920108. Work at University College, Cork, was supported by Forbairt Grant SC/94/227.

*Electronic address: merlin@umich.edu

- [1] For recent reviews, see S. Ruhman, A.G. Joly, and K.A. Nelson, *IEEE J. Quantum Electron.* **24**, 460 (1988); W.A. Kütt, W. Albrecht, and H. Kurz, *IEEE J. Quantum Electron.* **28**, 2434 (1992).
- [2] J.M. Chwalek *et al.*, *Appl. Phys. Lett.* **57**, 1696 (1990).
- [3] T.P. Dougherty *et al.*, *Science* **258**, 770 (1992).
- [4] T. Mishina *et al.*, *Phys. Rev. B* **46**, 4229 (1992).
- [5] H.J. Bakker, S. Hunsche, and H. Kurz, *Phys. Rev. Lett.* **69**, 2823 (1992).
- [6] P. Grenier *et al.*, *Phys. Rev. B* **47**, 1 (1993).
- [7] T.K. Cheng *et al.*, *Appl. Phys. Lett.* **62**, 1901 (1993).
- [8] D.P. Kien, J.C. Loulergue, and J. Etchepare, *Phys. Rev. B* **47**, 11 027 (1993).
- [9] A. Yamamoto *et al.*, *Phys. Rev. Lett.* **73**, 740 (1994).
- [10] D.A. Williams, *Phys. Rev. Lett.* **69**, 2551 (1992); S. Fahy and R. Merlin, *Phys. Rev. Lett.* **73**, 1122 (1994).
- [11] J.K. Kjems *et al.*, *Phys. Rev. B* **8**, 1119 (1973).
- [12] J.F. Scott, *Phys. Rev.* **183**, 823 (1969).
- [13] G. Yao *et al.*, *J. Mater. Res.* **7**, 1847 (1992), and references therein.
- [14] Y.R. Shen and N. Bloembergen, *Phys. Rev.* **137**, A1787 (1965).
- [15] See, e.g., Y.-X. Yan and K.A. Nelson, *J. Chem. Phys.* **83**, 5391 (1985); **87**, 6240 (1987), and references therein.
- [16] W. Hayes and R. Loudon, *Scattering of Light by Crystals* (Wiley, New York, 1978), Chap. 1.
- [17] R. Merlin (unpublished); for a discussion of boundary reflection in the related case of sum-frequency generation, see Y.R. Shen, *The Principles of Nonlinear Optics* (Wiley, New York, 1984), p. 73.
- [18] See, e.g., A.J. Taylor, D.J. Erskine, and C.L. Tang, *J. Opt. Soc. Am. B* **2**, 663 (1985).